ACS APPLIED MATERIALS & INTERFACES

Research Article

www.acsami.org

Reduction of the Water Wettability of Cellulose Film through Controlled Heterogeneous Modification

Wei Li, Yuehan Wu, Weiwei Liang, Bin Li, and Shilin Liu*

College of Food Science & Technology, Huazhong Agricultural University, Wuhan, Hubei, 430070, China

ABSTRACT: A facile method had been applied to introduce hydrophobic properties to cellulose materials by incorporation of polyurethane acrylate (PUA) prepolymers into the porous structured cellulose matrix through dip-coating; then, PUA prepolymers were cured around interconnected cellulose fibers under UV light, encapsulating a cellulose matrix with a hydrophobic polymer shell. The characterization of the composite films confirmed the success of the heterogeneous modification, and the chemical structure of the cellulose matrix was preserved. The composite films integrated the merits of cellulose and PUA resin, but the highly hydrophilic behavior of cellulose has been reduced. Contact angle measurements with water demonstrated that the composite films had obvious hydrophobic properties and an obvious reduction in the water uptake and the permeability toward water vapor gas at different relative humidity was also observed. The transmittance of the composite films at 550 nm was about 85%. The thermal and mechanical properties of the composite films were improved when compared with that of PUA resin. The obtained composite based on cellulose and UV curing technology was a good choice for the development of biomass materials with modified surface properties.

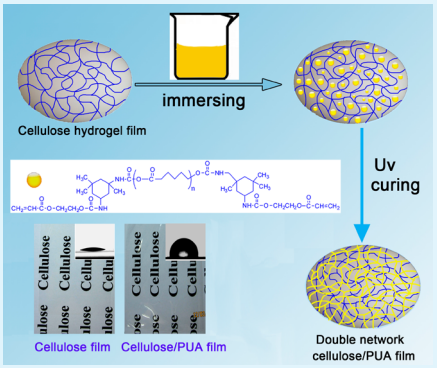

KEYWORDS: *cellulose, polyurethane acrylate, UV-curing, composite film*

1. INTRODUCTION

Biobased materials with high thermal, mechanical, and gas barrier properties as well as novel optical transparency are the principal ingredients of paper, packaging products, and food products, etc.[1−3] Cellophane, as a commercial film of regenerated cellulose, has the properties of high transparency, durability, and imperviousness to air, lipid, bacteria, and dirt in the dry state.[4] However, the properties of cellophane are sensitive to humidity, and it will change dramatically in the swollen state. Nevertheless, it lost its ground for conventional polymers in the last few decades due to the high cost for production and generated pollutants (CS_2 and H_2S). Thus, *N*-methylmorpholine-*N*-oxide hydrate (NMMO),[5] ionic liquids,[6] aqueous NaOH solution,[7] and alkali/urea solutions[8−10] have been developed as alternative solvents for the preparation of new cellulose materials, and the related fundamental and application studies have been extensively carried out. However, the native high hydrophilicity of cellulose plays an important role in limiting the usage of cellulose based materials.

Chemical modification of cellulose in both homogeneous[11−13] and heterogeneous conditions[14−16] has been performed for tailoring the important properties of cellulose for specific applications. Although many cellulose derivatives including methylcellulose, carboxymethycellulose, hydroxypropyl methylcellulose, cellulose sulfate, etc., have been developed and used widely, plentiful potential applications of cellulose derivatives are restricted by their hygroscopic properties, leading to change in the chemical structure of cellulose and then resulting in physical degradation such as swelling and loss of mechanical properties, fiber embrittlement, etc. On the other hand, the utilization of nanotechnology for large-scale preparation of functional cellulose materials was hindered because of the costs that mainly resulted from the complicated and sophisticated preparation process.[17−20] In many cases, processing required the use of a polar solvent or hydrophilic matrix due to the hydrophilicity of cellulose, and efficient hydrophobization of the nanofibrils remains a challenging task.

In our previous works, we have put intensive research into the development of functional materials based on cellulose, and we found that regenerated cellulose film prepared from LiOH/urea or NaOH/urea aqueous solution had the porous structure; it could be used as scaffolds for the synthesis of inorganic nanoparticles in situ.[21−25] Inspired by this interesting phenomenon, in this work, we presented a facile pathway and attempted to prepare cellulose composite film by incorporation of organic polyurethan acrylate (PUA) monomers in porous structured cellulose matrix and, then, cured it under UV light. Our approach was based on the impregnation of the porous structured cellulose film with PUA prepolymer solutions, and followed with dip coating. The proposed process based on UV-initiated polymerization of PUA prepolymers in the cellulose matrix and the formed PUA in the cellulose matrix changed the chemical structure of cellulose nanofibers network hardly. This

Received: January 16, 2014
Accepted: March 25, 2014
Published: March 25, 2014

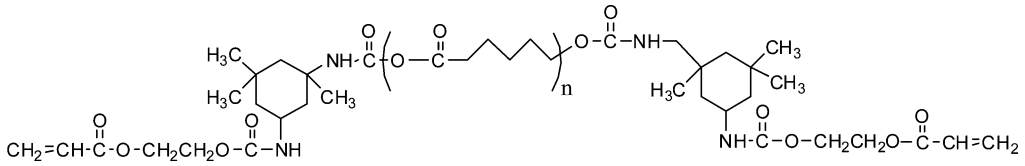

Figure 1. Chemical structure of the polyurethane acrylate prepolymer used in this work.

method was facile, and no waste liquid was generated during the preparation process. Moreover, the interesting properties (transparency, dimensional stability, etc.) of the cellulose were maintained, while the high hydrophilic properties, which often limit its applications, had been reduced. The structure and properties including mechanical, surface properties, and water vapor permeability of the composite films have been characterized and evaluated. The method presented herein was promising for the improvement waterproof properties of cellulose and without changing its chemical structure and also could be applied to other biomass routinely for the preparation of functional materials for specific applications.

2. EXPERIMENTAL SECTION

2.1. Materials. Native cellulose (cotton linter, α-cellulose ≥95%) was supplied by Hubei Chemical Fiber Co. Ltd. (Xiangfan, China), and its viscosity-average molecular weight (M_η) was about 1.07×10^5, which was determined in cadoxen at 25 °C.[26] Alphatic PUA was provided by Pengbo Co. Ltd. (Shanghai, China), and the structure is shown in Figure 1. Other chemicals with analytical grade were supplied by the Sinopharm Chemical Reagent Co. Ltd. (Shanghai, China).

2.2. Preparation of Regenerated Cellulose (RC) Film. The dissolving process for cellulose has been reported in our previous work.[21] Briefly, native cellulose was dispersed into aqueous LiOH/urea solution. It was then frozen at −20 °C to get a solid substance and then thawed at room temperature to obtain a transparent cellulose solution (5 wt %). After the bubbles in the cellulose solution was removed by centrifugation, the solution was cast on a glass plate with thickness about 1 mm and then immersed into anhydrous ethanol for coagulation and regeneration for 10 min. The RC films were washed with deionized water thoroughly, treated with acetone aqueous with different volume fractions to replace the water in the films, and then kept in absolute acetone before using.

2.3. Preparation of PUA/Cellulose Composite Film. The obtained pure RC films after being replaced the water with acetone were immersed in freshly prepared solutions containing PUA prepolymer and curing agent, which allowed the precursor solution to penetrate into the cellulose networks. The immersion time was controlled to be 8 h. The composite films were treated at 40 °C for the removal of solvent and then were exposed to UV light and cured for 5 min. The composite films were washed with acetone first and followed with water, and then they were dried at ambient conditions. The composite films prepared from PUA prepolymer with a concentration of 10, 25, 40, 55, and 70 wt % were coded as RC-PUA10, RC-PUA25, RC-PUA40, RC-PUA55, and RC-PUA70. Pure PUA film was prepared in a mold with the same conditions and was coded as PUA.

2.4. Characterization. Wide-angle X-ray diffraction (XRD) measurement was carried out on an XRD diffractometer (D8-Advance, Bruker, USA), the voltage and current during the test was 40 kV and 40 mA, respectively, and Cu Kα radiation with the weighted average λ of 0.15406 nm was used. Fourier-transform infrared (FT-IR) spectroscopies of the samples were characterized with an FT-IR spectrometer (FT-IR 615, Japan). The samples were ground into powders and dried in a vacuum drying oven at 50 °C for 36 h, then mixed with KBr, and pressed for the tests. Thermal gravimetric analysis (TGA) was carried out by using a thermogravimetric analyzer (TGA/DSC1/1100SF, Mettler Toledo). About 30 mg of the powder samples was used for each test, the test was conducted in a nitrogen atmosphere, and the test temperature ranged from 20 to 700 °C at a rate of 10 K·min^{-1}. The optical transmittance of the films was carried out on a UV−visible spectroscopy (F300s Ultraviolet lamp) from 300 to 800 nm using air as a reference, the thickness of the cellulose, polyurethane acrylate, and composite films was about 33 μm. The surface morphology of the samples was characterized by using scanning electron microscopy (SEM) (Hitachi S4800, Japan). The contact angle for water of the composite films was investigated by using a contact angle analyzer (DCA315, USA). Five contact angle measurements at different places were performed for each sample. The mechanical properties of the films were characterized with a tensile tester (CMT 6503, Shenzhen SANS Test machine Co. Ltd., China) according to ASTM/D638-91 with a speed of 5 mm·min^{-1}.

The equilibrium-swelling ratio (Q) of the films was characterized according to the reported method.[27] A piece of dry film with a known weight was kept in distilled water until it reached a swelling-equilibrium state at a constant temperature, and then, the water was wiped off from the surface and the sameple was weighed. The equilibrium-swelling ratio (Q) was calculated using the following equation:[27]

$$Q = \frac{W_h - W_d}{W_d} \tag{1}$$

Where, W_h was the weight of the swollen film and W_d was the weight of the dried sample. Five replicates for each sample were performed to obtain an average value of Q.

Water is a nonsolvent for cellulose and PUA, and it just can penetrate into the pores of the composite films. Thus, the pore volume (V_p, milliliters of pores in 1 g of film) of the samples was calculated through the uptake of water in the films by using the following formula:[28]

$$V_p = \frac{M_{wet} - M_{dry}}{\rho M_{dry}} \tag{2}$$

Where, M_{wet} was the weight of the samples immersed in water until it reached swelling-equilibrium. Here ρ was the density of water (0.995 g·mL^{-1}, 30 °C).

The cross-link density (V_e) of the samples was determined through the equilibrium swelling based on the Flory−Rehner theory.[28−31] In this theory, a phantom model was used to describe the elastic behavior of the swollen polymer network:

$$V_e = -\frac{\ln(1-\phi_r) + \phi_r + X\phi_r^2}{V_1\left(\phi_r^{1/3} - \frac{\phi_r}{2}\right)} \tag{3}$$

$$\phi_r = \frac{\frac{W_d - W_{ins}}{\rho_r}}{\frac{W_d - W_{ins}}{\rho_r} + \frac{W_{sol}}{\rho_s}} \tag{4}$$

Where, V_e was the network chain density (mol·cm^{-3}), χ was the Flory−Huggins interaction parameter (0.391), V_1 was the molar volume of acetone (75.76 cm^3·mol^{-1}), Φ_r was the PUA volume fraction, w_d and w_i were the deswollen and initial weights of the samples, respectively, ρ_r and ρ_s were the density of cured polyurethane acrylate (1.051 g·cm^{-3}) and acetone (0.767 g·cm^{-3}), respectively, and w_{sol} was the weight of the absorbed acetone after 72 h. Three replicates for each sample were carried out.

The water vapor transmission rate (WVTR) of the films was determined according to the ASTM E96-95 standard test method. Saturated aqueous solutions with different salts ($MgCl_2$, 31% of RH at

Scheme 1. Process for the Preparation of the Polyurethane Acrylate/Cellulose Films

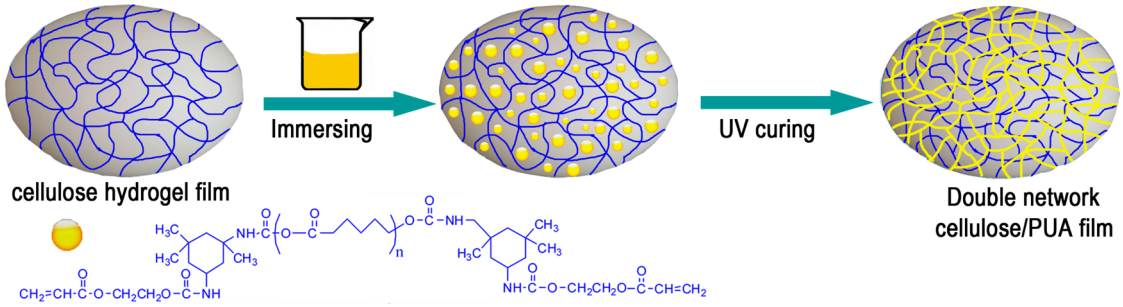

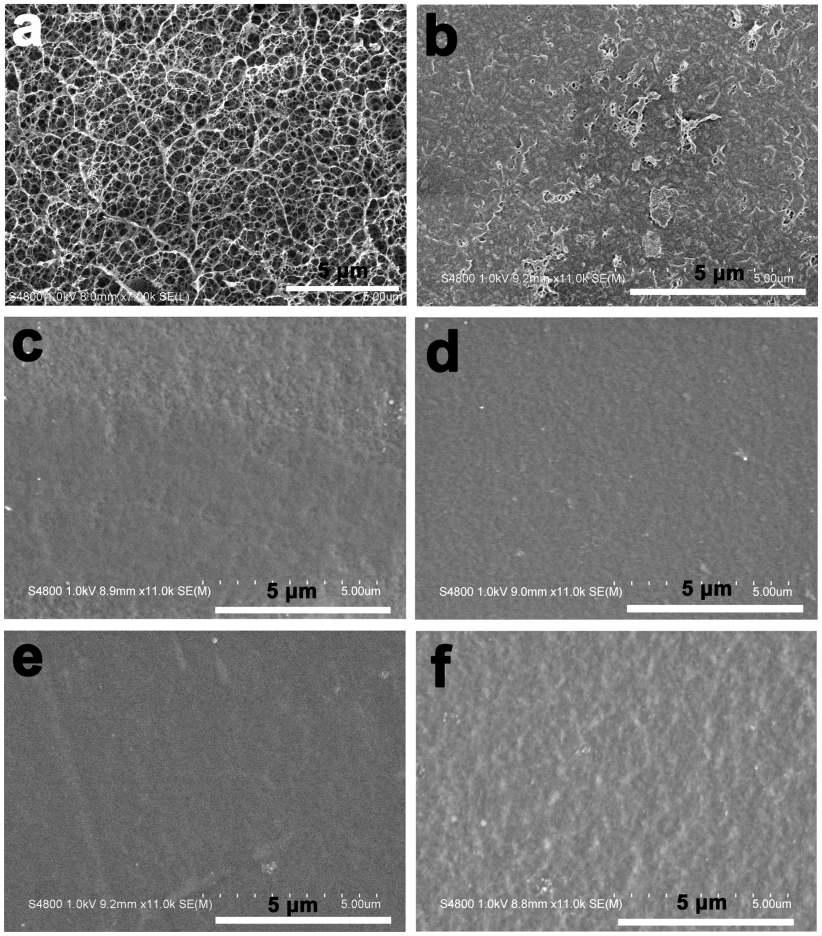

Figure 2. SEM images of the regenerated cellulose hydrogel film after being freeze-dried (a) and UV cured composite films prepared from polyurethane acrylate with different concentrations, RC-PUA10 (b), RC-PUA25 (c), RC-PUA40 (d), RC-PUA55 (e), and RC-PUA70 (f). The composite films were dried at ambient conditions.

25 °C; NaCl, 75% of RH at 30 °C) were used to establish different relative humidity (RH) inside the test chamber and weighing bottles were used in the test. 3 g anhydrous $CaCl_2$ was added to the weighing bottle to maintain 0% RH in the bottle headspace, the test film was placed over the mouth of the weighing bottle, and then, molten paraffin was applied to seal the film over the rim of the weighing bottle. The weighing bottle was placed in sealed jars containing saturated NaCl solution at 30 °C. The RH in the jar was kept by placing 1000 mL of distilled water in the bottom of the jar. The weighing bottle was weighed every 1 h for about 3 days. The amount of the water vapor that permeated through the film was determined from the increased weight of the weighing bottle. WVTR and water vapor permeability (WVP) were calculated from the following formula:[32]

$$\mathrm{WVTR} = \frac{\Delta w}{\Delta t A}$$

$$\mathrm{WVP} = \frac{\mathrm{WVTR}L}{\Delta p} \tag{5}$$

Where, WVTR was in grams per second squared meter, $\Delta w/\Delta t$ was rate of water gain in grams per hour, A was the exposed area of the film in squared meters, L was the mean thickness of samples in meters, Δp was the difference in partial water vapor pressure between the two sides of film in pascal. The water vapor pressure on the high-stream side of the film was 3.2 kPa (water vapor pressure of saturated NaCl aqueous solution at 30 °C), while inside the bottle it was assumed to be zero.

3. RESULTS AND DISCUSSION

The process for the preparation of the composite films was shown in Scheme 1. The cellulose hydrogel film at swollen state presented porous structure, comprising fibrils with diameters about 20 nm, as it was shown in Figure 2a. The porous structure was ascribed to the phase separation of the cellulose solution during the regeneration in ethanol, where polymer-rich and solvent-rich regions were formed, and the solvent-rich regions contributed to the formation of the pores. The cellulose hydrogel film was a transparent material with water content about 92% and porosity about 95%, and the S_{BET} of the freeze-dried cellulose hydrogel film was about 270 $m^2 \cdot g^{-1}$. When the cellulose film was immersed into PUA prepolymer solution, the prepolymer could readily permeate into the cellulose matrix through the pores by diffusion. After being UV cured, the PUA prepolymers were cross-linked with each other directly in the cellulose matrix and a new network consisting of PUA was formed. Figure 2b–f shows the surface morphologies of the composite films after being dried at ambient conditions. The surface of the composite film prepared from the prepolymer solution with lower concentration (≤10 wt %) was rough, indicating the incorporated content of the prepolymer was not enough for filling the pores of the cellulose matrix, because of the effect of the diffusion equilibrium. For the composite films prepared from the PUA prepolymer with concentration higher than 10 wt %, but lower than 55 wt %, the surface was smoother. This indicated that the concentration of the prepolymer had an effect on the microstructure of the composites. For the composite films prepared from higher concentration, the prepolymer was deposited on both cellulose nanofibrils and pores of the cellulose matrix, and then, it formed films after being cured with UV light. It must be mentioned that light curing efficiency also had an important influence on the surface morphology of the composites and pure PUA film. When the PUA prepolymer in the cellulose matrix was higher, in the given exposure time under the UV light, some prepolymer was not cured, and it was removed after the wash with acetone; therefore, the surface was rough, as shown in Figure 2f. Compared with the surface morphology of the composites, RC film dried at ambient conditions was also smooth. The different wetting performance of the composite films indicated that the PUA resin had been loaded in the cellulose matrix.

The successful loading of PUA resin in the cellulose matrix was clearly confirmed by FT-IR analyses, as shown in Figure 3a. One significant difference between the RC and PUA was the O–H stretch vibrations in the 3200–3600 cm^{-1} region. The O–H stretch band of RC was inherently broad, reflecting the complexity of hydrogen bond networks in RC as well as water molecules present in the amorphous region.[33] The weakened or disappeared peak at 1650 cm^{-1} which was associated with the water in cellulose suggested the hydrophobicity of the composite films had been improved. The strong bands near 2900 cm^{-1} could be ascribed to the C–H stretch vibrations. While for the composite films, it shifted to higher wavenumbers, the shoulder peaks in the lower (2860 cm^{-1}) and higher (2940 cm^{-1}) energy sides of the C–H peak could be assigned to the symmetric and asymmetric CH_2 stretch vibrations of the PUA, respectively. It indicated there was no chemical interaction between cellulose and PUA. For PUA film, the strong absorption peak at 3363 cm^{-1} was assigned to the NH stretching vibration. This resulted from the hydrogen

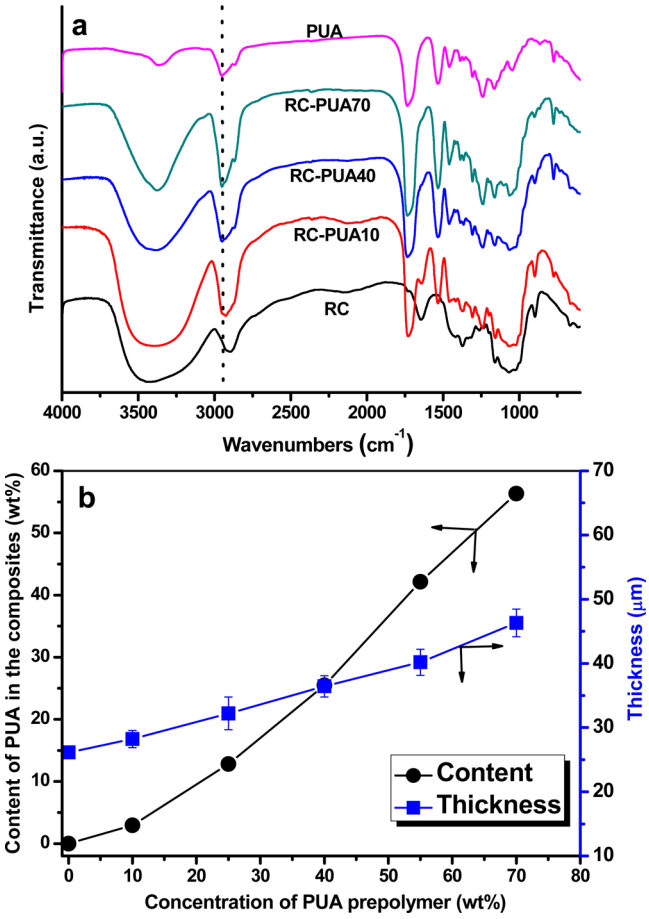

Figure 3. FT-IR spectra of the regenerated cellulose (RC) film, PUA, and some composite films (a) and the influence of the concentration of polyurethane acrylate on the weight of PUA and thickness of the composite films after UV curing (b).

bonding between NH and carbonyl groups of PUA, indicating the increased cohesion between the hard and soft segments of the PUA. The remarkable peak at 1722 cm^{-1} was correlated with the stretching vibration of both urethane and ester carbonyl.[34] This indicated that there was no phase separation between hard and soft segments in the PUA matrix. The peak of the carbonyl stretching vibration hardly shifted in the composite films, suggesting that the hydrogen bonding between NH and C═O was not disturbed by the cellulose matrix. The content of PUA in the composite films increased with the increasing concentration of the prepolymer, and the thickness of the composite films increased slightly with the incorporated PUA resin, as shown in Figure 3b; the higher concentration of PUA prepolymer used, the more PUA resin would be incorporated in the cellulose matrix. This demonstrated that the porous structured cellulose matrix was a novel scaffold for the incorporation of prepolymer for the modification of the properties of the matrix and that the content of the resin in cellulose could be controlled by changing the concentration of PUA prepolymer used, which was very important for adjusting the properties of the cellulose based composites.

The thermal stability of the composites was investigated by using thermogravimetry in N_2 atmosphere. As shown in Figure 4a, all the samples exhibited an excellent heat-resistance up to at least 300 °C. There was a small weight loss of ~5% below 100 °C for the composite films; it resulted from the release of

dx.doi.org/10.1021/am500341s | ACS Appl. Mater. Interfaces 2014, 6, 5726–5734

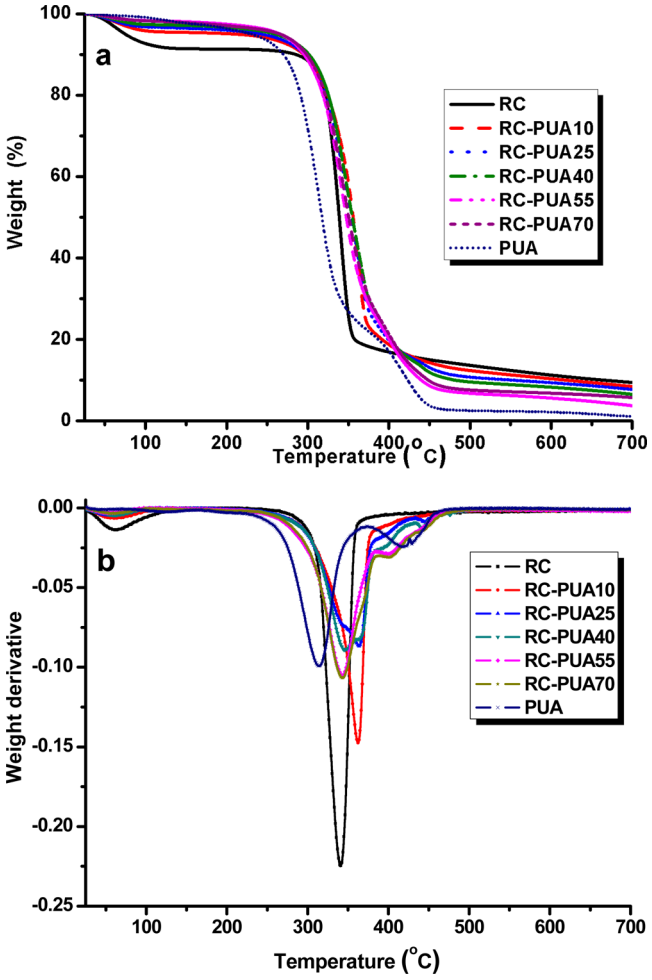

Figure 4. Thermal analysis of the RC, PUA, and composite films (a), TG-DTA curves with the weight loss and exoendothermal reaction of the films with different resin content (b).

moisture from the samples. While for the regenerated cellulose film, the weight loss in the same temperature region was about 10%, indicating an increase in hydrophobicity of the composite films after loading of PUA resin. With the elevating temperature, the pure RC film showed an obvious weight loss in the temperature range from 300 to 350 °C, it was the temperature of cellulose in N_2. Pure PUA had a poorer thermal stability than that of the RC film, and the loaded PUA in cellulose matrix had a positive influence on the thermal stability of the composites. The thermal stability of the composites containing less than 25 wt % PUA resin was shown in Figure 4a; the decomposition temperature was higher than that of RC, with the increasing content of PUA in cellulose matrix, the decomposition temperature decreased. There were significant differences in residues (Figure 4a). The composite residues presented fewer residues than RC and more than PUA film; this suggested that the PUA film was a protective layer, and the thermostability of the composites were improved. The thermal stability of the composite films was higher than that of PUA, as shown in Figure 4b.

The transmittance of the RC, PUA, and composite films were shown in Figure 5. The RC film and PUA were optically transparent, and their transmittances were about 88% in the wavelength range 400−800 nm. The composite films had transmittance about 88−85% in the same wavelength range,

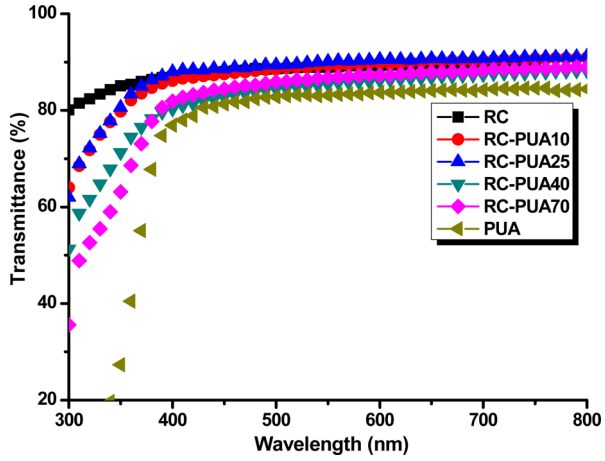

Figure 5. Optical transmittance spectra of RC, PUA, and composite films in the wavelength from 300 to 800 nm.

and the composite films containing PUA resin with content lower than 13 wt % had improved transmittance over that of RC film. The transmittance of the composites decreased slightly with the increasing of the PUA resin content in cellulose matrix, while the transmittance of the composite films was improved when compared with that of the PUA film. The difference in the refractive index (RI) of the cellulose and the PUA resin had an influence on the transmittance of the composites. It was well-known that for a transparent polymer composite, the optical property was described using the following formula:[35]

$$\frac{I}{I_0} \equiv \exp\left[-\frac{V_p \chi r^3}{4\lambda^4}\left(\frac{n_p}{n_m} - 1\right)\right]$$

Where, χ was the optical path length, V_p was the filler volume fraction, r was the filler radius, λ was the light wavelength, and n_p and n_m were the refractive indices of the fillers and matrix, respectively. The refractive indexes of cellulose and PUA are about 1.54 and 1.44, respectively. It has been reported that the difference in the refractive index of the filler and matrix had an influence on controlling the optical transmittance of the composite films. The composite films containing higher content of PUA resin would have poor light transmittance, for light refraction and reflection would happen at the interfaces between cellulose and PUA. It has also been reported that the transmittance of cellulose acetate/epoxy resin composite films decreased with increasing content of epoxy resin.[36] Moreover, the surface reflection also had a negative impact on the transmittance of the composite films that resulted from the difference in the RIs. The relationship between light reflection and RI was described by using the following equation:[37]

$$\Gamma = [(n_R - n_F)/(n_R + n_F)]^2$$

Where, Γ was the reflective coefficient and n_R and n_F were RIs of PUA and cellulose, respectively. Therefore, the higher the difference bewteen RIs of the PUA and cellulose, the higher the reflective coefficient obtained for the composites. With the incorporation of PUA resin into the cellulose matrix, the cellulose/air interfaces were replaced by three types of interfaces, i.e., cellulose/PUA resin, cellulose/air, and PUA/air resin in the composite films. FT-IR results indicated that there was no chemical interaction between cellulose and PUA; the increased interfaces would have a negative influence on the

dx.doi.org/10.1021/am500341s | ACS Appl. Mater. Interfaces 2014, 6, 5726−5734

transmittance of the composite films. However, on the other hand, the incorporated PUA resin had an effect on the microstructure of the composites, resulting in a denser structure for the composite films. The diffuse reflection of the light in the films decreased. Therefore, the composite films would have good optical transmittance. Although there were many factors that would affect the optical transmittance of the material, the transmittance of a composite could be improved when the light reflection at the interfaces was reduced to a large extent. Cellulose films have good optical transmittance and can be used as optically functional materials; water sensitivity is a crucial aspect of cellulose based composites because the moisture picked up upon immersion in water or in high humidity environments is detrimental to their mechanical strength and dimensional stability. Thus, we investigated the relationship between the content of resin and the moisture absorption of the composites to minimize hygroscopicity.

Figure 6a shows the water uptake of the RC and composite films as a function of the immersing time. All the materials had

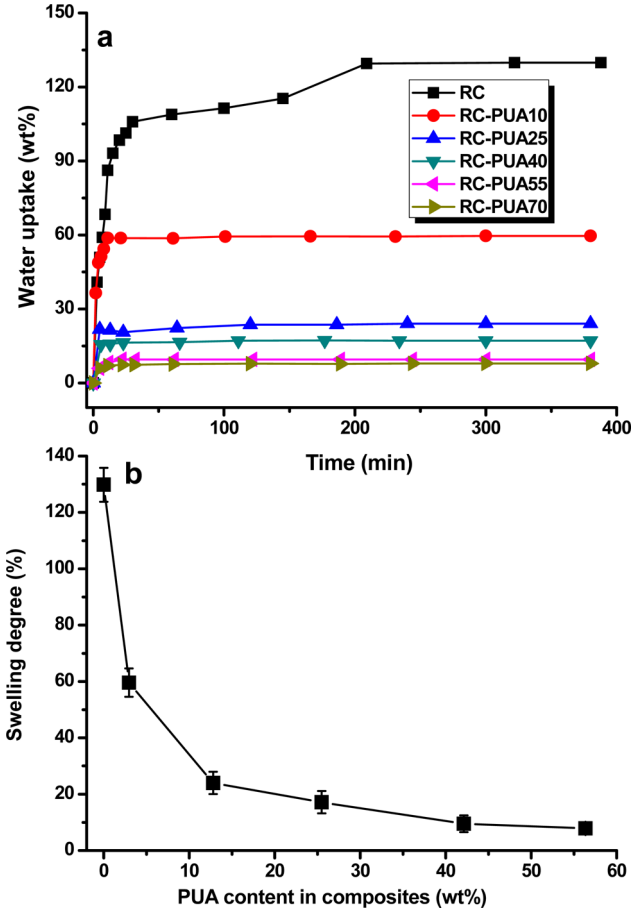

Figure 6. Comparison of water uptake ability of the films with different content of loaded polyurethane acrylate (a) and the effects of polyurethane acrylate content on the swelling degree of the films (b).

a fast water uptake within 0.5 h, following similar patterns. The composite films had an obvious lower water uptake behavior than that of pure RC film. RC film had a swelling degree of about 129%, which often limited its uses. The swelling degree decreased to 59% for the composite film containing PUA with content only about 2.9 wt %, the swelling degree of the composites decreased with the increase of the content of PUA resin, as shown in Figure 6b. PUA resin has hydrophobic characteristics based on its molecular structure, which contributed to the hydrophobic performance of the composites. Furthermore, the cross-linked PUA resin in the cellulose matrix would result in the reduction of the absorbed water and the restriction of the movement of the molecular chain during the swelling process. Therefore, the hydrophobic properties of the composite films were improved.

The composite films also had low water vapor permeability, and the results were shown in Figure 7. The incorporated PUA

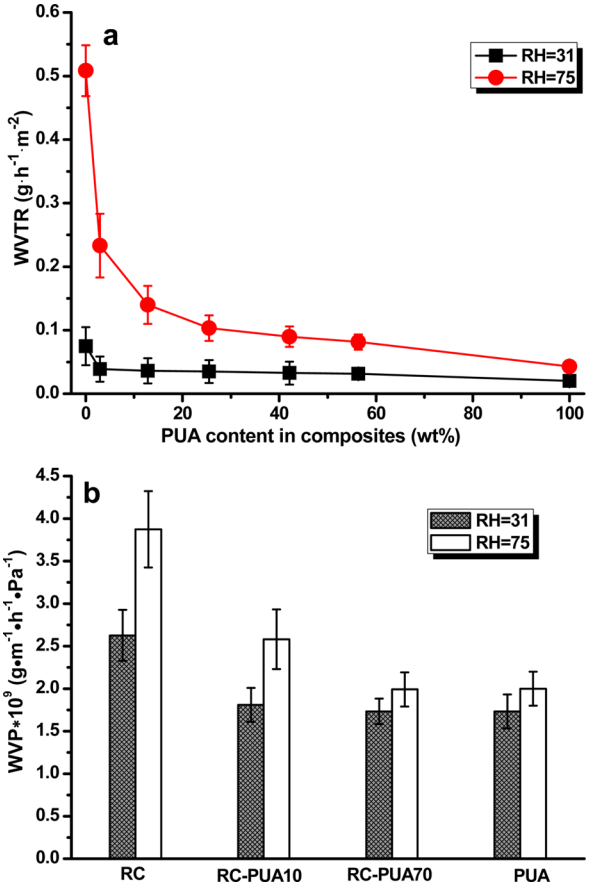

Figure 7. Water vapor transmission rate (WVTR) (a) and water vapor permeability (WVP) (b) values of the composite films with different contents of loaded polyurethane acrylate.

resin in the cellulose matrix had an obvious influence on the water vapor permeability of the composites. The WVP value of RC film was about 3.9×10^{-9} g·m^{-1}·h^{-1}·Pa^{-1} while that of the RC-PUA70 composite film was just 2.0×10^{-9} g·m^{-1}·h^{-1}·Pa^{-1} under a humidity of 75%, which showed almost 50% reduction; this suggested that the hydrophobicity of the cellulose film had been improved by the loading of PUA resin. The permeability toward water vapor of RC and composite films increased with increasing relative humidity. It has been reported that the migration of a water molecule through hydrophilic polymers (e.g., starch) was complicated during the water sorption isotherms and the absorbed water had an important influence on it.[38] When the RH was lower than 40%, water molecules were often absorbed in the amorphous section of a material, where hydrogen bond active sites were the main ingredients. While for higher RH (>70%), water clusters were formed and the solubility of the water vapor increased drastically, resulting

dx.doi.org/10.1021/am500341s | ACS Appl. Mater. Interfaces 2014, 6, 5726−5734

in a plasticization effect, which would have a dramatic increase in the permeability toward water vapor;[39] therefore, the humidities had an influence on the permeability toward water vapor, as shown in Figure 7a.

The incorporated PUA resin had an influence on the static free volumes of the composites, as shown in Figure 8a; the total

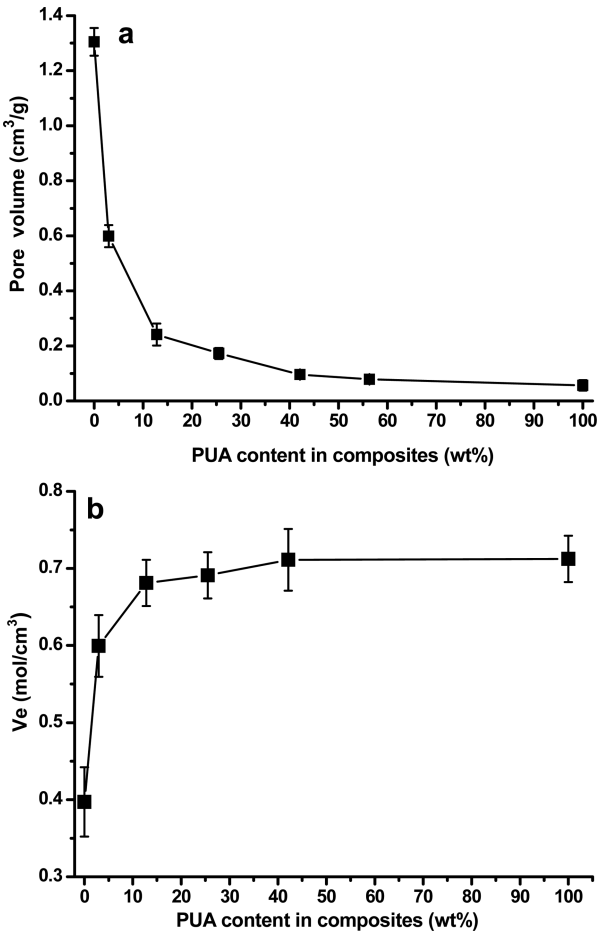

Figure 8. Total volume of pores in the composite films estimated from the uptake of water shown as a function of polyurethane acrylate content (a) and the degree of crosslink (V_e) of the composite films as a function of polyurethane acrylate content (b).

volume of pores (V_p) of the composite films was plotted against the PUA resin content. The V_p of pure cellulose film and the PUA film was about 1.3 and 0.057 $cm^3 \cdot g^{-1}$, respectively. The incorporated PUA resin has an obvious influence on the V_p of the composites. For the composite containing only about 2.9 wt % PUA, the V_p decreased to about 0.6 $cm^3 \cdot g^{-1}$ and the corresponding cross-link degree increased to 0.59 $mol \cdot cm^3$. The V_p of the composite films decreased and reached a plateau gradually with the increasing content of PUA in a cellulose matrix; on the contrary, the corresponding cross-link degree of the composite films increased. According to the swelling behaviors of the composite films, the values, regarding Q and V_p, were lower, which suggested that effective cross-links were happened between PUA resin, leading to a restriction on the movement of the molecular chain. Therefore, the swelling capacity of the composites containing PUA resin was decreased. The cross-link densities (V_e) of the composites increased with the increasing the PUA resin content in the cellulose matrix, as shown in Figure 8b. The increased V_e of the composites, the decreased swelling degree would have, further supported the results shown in Figures 6 and 8a.

The surface energy of composite films could be determined from the measurement of the contact angles formed by water on their surface. Figure 9 shows the average contact angle of

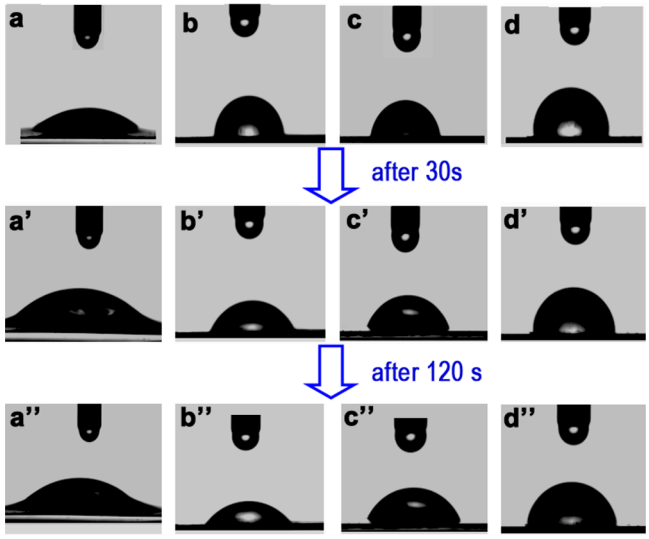

Figure 9. Contact angle data of water droplets on RC (a, a′, a″) and RC-PUA10 (b, b′, b″), RC-PUA40 (c, c′, c″), and RC-PUA70 (d, d′, d″). Photographs were taken immediately after the droplets were applied, 30 s (′), and 120 s (″) later.

water deposited onto the surface of the composite films. The water droplet angles of the RC film changed immediately with the absorption of the droplet by the RC film within 2 min. The contact angle for water of the composite films with the content of PUA resin only about 2.9 wt % improved remarkably. Furthermore, the volume of the water droplets changed hardly on the surface of the composite films during the testing process, indicating no observed absorption of water happening to the composite films. With the increasing content of PUA resin in the cellulose matrix, the contact angle for water of the composite materials increased, as shown in Figure 10. This indicated that the decrease in the surface energy of the composite films was mostly reduced by the loading of PUA resin.

The mechanical behavior of the RC, PUA, and the composite films was investigated by using tensile testing at room temperature. Figure 11 shows the stress−strain curves of the materials. PUA displayed a nonlinear elastic behavior and possessed a low tensile strength of 21 MPa and a low tensile modulus of about 15 MPa. With the decreasing of PUA resin in the cellulose matrix, the tensile strength of the composite films increased significantly from 21 MPa (PUA) to 82 MPa (for RC-PUA10), and the elongation at break of the composites decreased from 85% (PUA) to 15% (for RC-PUA10). This indicated that the incorporated PUA into the cellulose matrix resulted in strong interactions between the cellulose networks and PUA networks. The Young's modulus of the composite films increased nearly exponentially when compared with that of the PUA films. Especially, the Young's modulus of RC-PUA10 was about 250 times higher than that of PUA. This resulted from the enforcing effect of the rigid network of cellulose. This indicated that the composite films integrated the merits of cellulose and PUA resin. In terms of a comprehensive

dx.doi.org/10.1021/am500341s | ACS Appl. Mater. Interfaces 2014, 6, 5726−5734

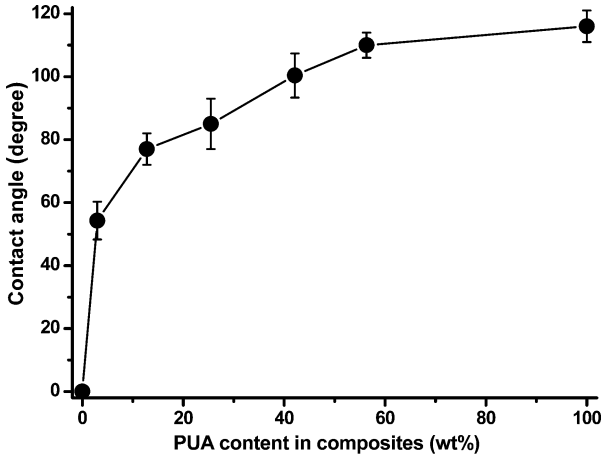

Figure 10. Effects of the polyurethane acrylate content on the contact angles of the composite films.

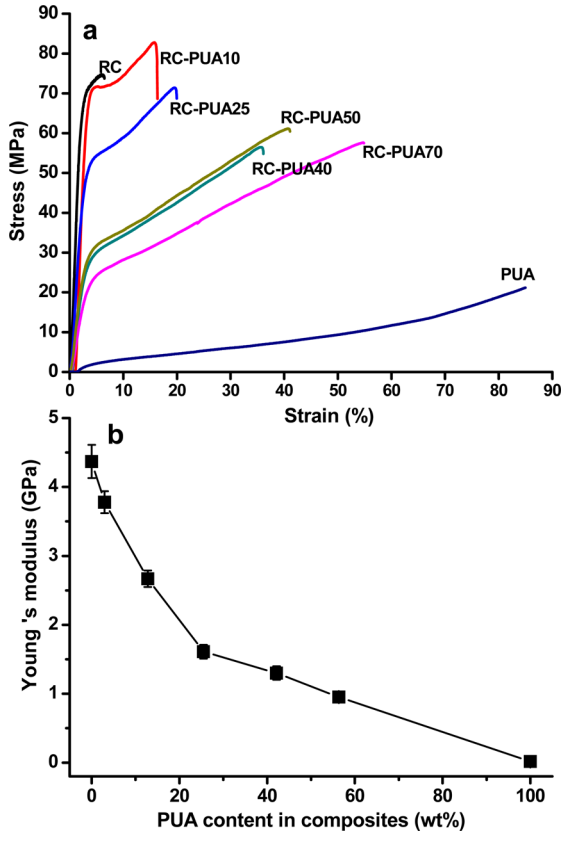

Figure 11. Tensile stress−strain behaviors of the RC, PUA, and composite films (a) and effect of varying polyurethane acrylate content in comparison with Young's modulus values of the films (b).

consideration, the optimal content of PUA resin in the cellulose ranged from 2 to 13 wt % and was the optimal proportion for the preparation of composite films with good mechanical, hydrophobic, and preferable gas barrier properties. The obtained composite films would have practical applications in paper, packaging products, and food products.

4. CONCLUSION

Transparent and bendable cellulose composite films had been prepared by dip coating of PUA prepolymer into the cellulose matrix and then UV curing. The composite films integrated the merits of cellulose and PUA resin, but the highly hydrophilic behavior of cellulose had been reduced. The swelling degree of the composites decreased with the increasing content of PUA resin. Contact angle measurements with water demonstrated that the composite films had obvious hydrophobic properties, and a decrease in the water uptake and the permeability toward water vapor gas at different relative humidity was also observed. The composite films had good mechanical properties, and the young's modulus decreased with the increasing content of PUA in the composites. In terms of a comprehensive consideration, the content of the resin in the cellulose matrix ranged from 2 to 13 wt % and was the optimal proportion for the preparation of composite films with good mechanical, hydrophobic, and preferable gas barrier properties, and the obtained biobased composite films are promising as waterproof materials.

AUTHOR INFORMATION

Corresponding Author

*E-mail: slliu2013@mail.hzau.edu.cn.

Notes

The authors declare no competing financial interest.

ACKNOWLEDGMENTS

This work was supported by the National Natural Science Foundation of China (No. 51273085 and 51003043) and project 2014PY024 by the Fundamental Research Funds for the Central Universities. We are also very thankful for Dr. Bakht Ramin Shah for checking the grammar.

REFERENCES

(1) Chou, C. T.; Yu, P. W.; Tseng, M. H.; Hsu, C. C.; Shyue, J. J.; Wang, C. C.; Tsai, F. Y. Transparent Conductive Gas-Permeation Barriers on Plastics by Atomic Layer Deposition. *Adv. Mater.* **2013**, *25*, 1750−1754.

(2) Huang, J.; Zhu, H. L.; Chen, Y. C.; Preston, C.; Rohrbach, K.; Cumings, J.; Hu, L. B. Highly Transparent and Flexible Nanopaper Transistors. *ACS. Nano.* **2013**, *7*, 2106−2113.

(3) Hsu, S. H.; Chang, Y. L.; Tu, Y. C.; Tsai, C. M.; Su, W. F. Omniphobic Low Moisture Permeation Transparent Polyacrylate/Silica Nanocomposite. *ACS Appl. Mater. Interfaces* **2013**, *5*, 2991−2998.

(4) Paunonen, S. Strength and Barrier Enhancements of Cellophane and Cellulose Derivative Films: A Review. *Bioresources.* **2013**, *8*, 3098−3121.

(5) Rosenau, T.; Potthast, A.; Adorjan, I.; Hofinger, A.; Sixta, H.; Firgo, H.; Kosma, P. Cellulose solutions in N-methylmorpholine-N-oxide (NMMO) − degradation processes and stabilizers. *Cellulose* **2002**, *9*, 283−291.

(6) Swatloski, R. P.; Spear, S. K.; Holbrey, J. D.; Rogers, R. D. Dissolution of Cellose with Ionic Liquids. *J. Am. Chem. Soc.* **2002**, *124*, 4974−4975.

(7) Roy, C.; Budtova, T.; Navard, P.; Bedue, O. Structure of Cellulose−Soda Solutions at Low Temperatures. *Biomacromolecules.* **2001**, *2*, 687−693.

(8) Liu, S.; Zeng, J.; Tao, D.; Zhang, L. Microfiltration performance of regenerated cellulose membrane prepared at low temperature for wastewater treatment. *Cellulose* **2010**, *17*, 1159−1169.

(9) Mao, Y.; Zhou, J.; Cai, J.; Zhang, L. Effects of coagulants on porous structure of membranes prepared from cellulose in NaOH/urea aqueous solution. *J. Membr. Sci.* **2006**, *279*, 246−255.

(10) Zhou, J.; Chang, C.; Zhang, R.; Zhang, L. Hydrogels Prepared from Unsubstituted Cellulose in NaOH/Urea Aqueous Solution. *Macromol. Biosci.* **2007**, *7*, 804−809.

(11) Li, Q.; Zhou, J.; Wu, P.; Zhang, L. Structure and solution properties of cyanoethyl celluloses synthesized in LiOH/urea aqueous solution. *Cellulose* **2012**, *19*, 161−169.

(12) Zhang, L.; Li, Q.; Zhou, J.; Zhang, L. Synthesis and Fluorescent Properties of Carbazole-Substituted Hydroxyethylcelluloses. *Macromol. Chem. Phys.* **2012**, *213*, 57−63.
(13) Song, Y.; Zhang, J.; Gan, W.; Zhou, J.; Zhang, L. Flocculation Properties and Antimicrobial Activities of Quaternized Celluloses Synthesized in NaOH/Urea Aqueous Solution. *Ind. Eng. Chem. Res.* **2010**, *49*, 1242−1246.
(14) Aulin, C.; Karabulut, E.; Tran, A.; Wagberg, L.; Lindstrom, T. Transparent Nanocellulosic Multilayer Thin Films on Polylactic Acid with Tunable Gas Barrier Properties. *ACS Appl. Mater. Interfaces* **2013**, *5*, 7352−7359.
(15) Ben Mabrouk, A.; Ferraria, A. M.; do Rego, A. M. B.; Boufi, S. Highly transparent nancomposite films based on polybutylmethacrylate and functionalized cellulose nanocrystals. *Cellulose* **2013**, *20*, 1711−1723.
(16) He, M.; Xu, M.; Zhang, L. Controllable Stearic Acid Crystal Induced High Hydrophobicity on Cellulose Film Surface. *ACS Appl. Mater. Interfaces* **2013**, *5*, 585−591.
(17) Quero, F.; Nogi, M.; Yano, H.; Abdulsalami, K.; Holmes, S. M.; Sakakini, B. H.; Eichhorn, S. J. Optimization of the Mechanical Performance of Bacterial Cellulose/Poly(l-lactic) Acid Composites. *ACS Appl. Mater. Interfaces* **2010**, *2*, 321−330.
(18) Ifuku, S.; Tsuji, M.; Morimoto, M.; Saimoto, H.; Yano, H. Synthesis of Silver Nanoparticles Templated by TEMPO-Mediated Oxidized Bacterial Cellulose Nanofibers. *Biomacromolecules.* **2009**, *10*, 2714−2717.
(19) Nogi, M.; Iwamoto, S.; Nakagaito, A. N.; Yano, H. Optically Transparent Nanofiber Paper. *Adv. Mater.* **2009**, *21*, 1595−1598.
(20) Rojas, O. J.; Lokanathan, A. R.; Kontturi, E.; Laine, J.; Bock, H. The unusual interactions between polymer grafted cellulose nanocrystal aggregates. *Soft. Matter.* **2013**, *9*, 8965−8973.
(21) Liu, S.; Tao, D. D.; Yu, T. F.; Shu, H.; Liu, R.; Liu, X. Y. Highly flexible, transparent cellulose composite films used in UV imprint lithography. *Cellulose* **2013**, *20*, 907−918.
(22) Liu, S.; Zhang, L. Effects of polymer concentration and coagulation temperature on the properties of regenerated cellulose films prepared from LiOH/urea solution. *Cellulose* **2009**, *16*, 189−198.
(23) Liu, S.; Zhang, L.; Zhou, J.; Wu, R. Structure and Properties of Cellulose/Fe_2O_3 Nanocomposite Fibers Spun via an Effective Pathway. *J. Phys. Chem. C* **2008**, *112*, 4538−4544.
(24) Liu, S.; Zhang, L.; Sun, Y.; Zhang, X.; Zhang, L.; Nishiyama, Y. Supramolecular Structure and Properties of High Strength Regenerated Cellulose Films. *Macromol. Biosci.* **2009**, *9*, 29−35.
(25) Liu, S.; Zhang, L.; Zhou, J.; Xiang, J.; Sun, J.; Guan, J. Fiberlike Fe2O3Macroporous Nanomaterials Fabricated by Calcinating Regenerate Cellulose Composite Fibers. *Chem. Mater.* **2008**, *20*, 3623−3628.
(26) Cai, J.; Liu, Y.; Zhang, L. Dilute solution properties of cellulose in LiOH/urea aqueous system. *J. Polym. Sci. Polym. Phys.* **2006**, *44*, 3093−3101.
(27) Bell, C.; Peppas, N. Water, solute and protein diffusion in physiologically responsive hydrogels of poly(methacrylic acid-g-rthylene glycol). *Biomaterials* **1996**, *17*, 1203−1218.
(28) Pojanavaraphan, T.; Liu, L.; Ceylan, D.; Okay, O.; Magaraphan, R.; Schiraldi, D. A. Solution Cross-Linked Natural Rubber (NR)/Clay Aerogel Composites. *Macromolecules* **2011**, *44*, 923−931.
(29) Valentín, J. L.; Mora-Barrantes, I.; Carretero-González, J.; López-Manchado, M. A.; Sotta, P.; Long, D. R.; Saalwächter, K. Novel Experimental Approach To Evaluate Filler−Elastomer Interactions. *Macromolecules* **2010**, *43*, 334−346.
(30) Pojanavaraphan, T.; Magaraphan, R. Prevulcanized natural rubber latex/clay aerogel nanocomposites. *Eur. Polym. J.* **2008**, *44*, 1968−1977.
(31) Pojanavaraphan, T.; Schiraldi, D. A.; Magaraphan, R. Mechanical, rheological, and swelling behavior of natural rubber/montmorillonite aerogels prepared by freeze-drying. *Appl. Clay. Sci.* **2010**, *50*, 271−279.
(32) Toméa, L. C.; Goncalvesa, C. M. B.; Boaventurab, M.; Brandãb, L.; Mendesb, A. M.; Silvestrea, A. J. D.; Netoa, C. P.; Gandinia, A.; Freirea, C. S. R.; Marrucho, I. M. Preparation and evaluation of the barrier properties of cellophane membranes modified with fatty acids. *Carbohydr. Polym.* **2011**, *83*, 836−842.
(33) Barnette, A. L.; Bradley, L. C.; Veres, B. D.; Schreiner, E. P.; Park, Y. B.; Park, J.; Park, S.; Kim, S. H. Selective Detection of Crystalline Cellulose in Plant Cell Walls with Sum-Frequency-Generation (SFG) Vibration Spectroscopy. *Biomacromolecules* **2011**, *12*, 2434−2439.
(34) Cao, X.; Dong, H.; Li, C. M. New Nanocomposite Materials Reinforced with Flax Cellulose Nanocrystals in Waterborne Polyurethane. *Biomacromolecules* **2007**, *8*, 899−904.
(35) Althues, H.; Henle, A.; Kaskel, S. Functional inorganic nanofillers for transparent polymers. *Chem. Soc. Rev.* **2007**, *36*, 1454−1465.
(36) Liao, H.; Wu, Y.; Wu, M.; Zhan, X.; Liu, H. Aligned electrospun cellulose fibers reinforced epoxy resin composite films with high visible light transmittance. *Cellulose* **2012**, *19*, 111−119.
(37) Tang, C. Y.; Liu, H. Q. Cellulose nanofiber reinforced poly(vinyl alcohol) composite film with high visible light transmittance. *Compos. Part A* **2008**, *39*, 1638−1643.
(38) Morillon, V.; Debeaufort, F.; Capelle, M.; Blond, G.; Voilley, A. Influence of the Physical State of Water on the Barrier Properties of Hydrophilic and Hydrophobic Films. *J. Agric. Food. Chem.* **2000**, *48*, 11−16.
(39) Vachoud, L.; Zydowicz, N.; Domard, A. Sorption and desorption studies on chitin gels. *Int. J. Biol. Macromol.* **2001**, *28*, 93−101.